

COMPUTATIONAL AEROELASTICITY IN HIGH PERFORMANCE AIRCRAFT FLIGHT LOADS*

Mike Love, Tony De La Garza, Eric Charlton, Dan Egle
Lockheed Martin Aeronautics Company

Keywords: *computational aeorelasticity, CFD, flight loads*

Abstract

A computational aeroelasticity method has been developed that combines a computational fluid dynamics (CFD) code based on a finite volume, Cartesian / prismatic grid scheme with automated unstructured grid creation and adaption with established structural finite element methods. This analysis is motivated by the need to develop an analysis capability for fighter-aircraft critical flight loads. Flight conditions for such often reside in transonic flow regimes and comprise nonlinear aerodynamics due to shocks, flow-separation onset, and complex geometry. The Multidisciplinary Computational Environment, MDICE [1], is providing for timely integration of Lockheed Martin's CFD software, SPLITFLOW [2] in a maintenance friendly, loosely coupled nonlinear analysis method. Analysis correlation with static aeroelastic wind tunnel data demonstrates potential. Analysis set-up and results for a fighter aircraft with multiple control surfaces are demonstrated.

1 Introduction

Computational aeroelasticity, or computational fluid dynamics (CFD) based aeroelasticity, is an emerging technology with high potential for the development of critical flight loads (Figure 1). The structural design of flight vehicles is highly dependent on the timeliness of accurate design flight loads. Flight loads are typically derived by combining aerodynamic loads, vehicle inertia, structural flexibility, and flight control laws

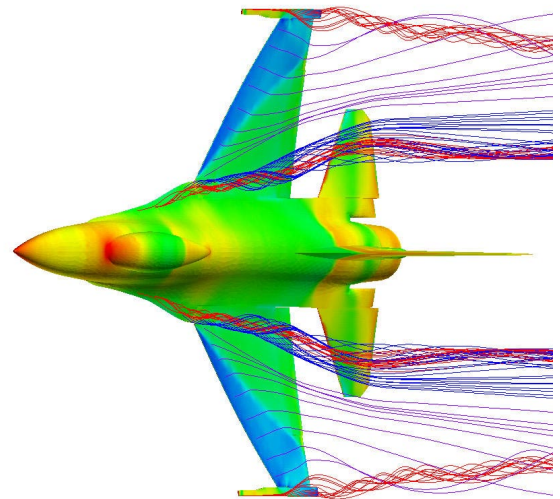


Figure 1: Pressures and streamlines obtained from a computational aeroelastic maneuver simulation

in maneuver simulations. The Loads engineer's time is mostly consumed in the assembly of accurate data for the maneuver simulation. Adequate characterization of vehicle aerodynamics is critical. Recent tool and technology developments are facilitating the aerodynamic characterization task of integrating data from CFD methods, wind tunnel testing and other aerodynamic methods to assemble an aerodynamic pressure database [3, 4]. This database is augmented by static aeroelastic analyses to account for flexibility effects of the structure and inertial effects of the flight vehicle. These analyses are performed at a distributed set of Mach number and altitude combinations. Historically, a linear static aeroelastic solution is acquired for each nonlinear rigid aerodynamic data set using linear aerodynamic panel methods. Linear methods do not

* Copyright © 2000 Lockheed Martin Corporation All rights reserved. Published by the International Council of Aeronautical Sciences with permission.

capture nonlinear phenomenon such as flow separation and moving shocks in the critical loads flight regime.

Figure 2 illustrates the construction and topology of a database for fighter loads. Literally thousands of aerodynamic pressure vectors are constructed over a distribution of Mach numbers, altitudes, and control parameter angles. The database is considered nonlinear because the integrated aerodynamic load coefficients (e.g., lift coefficient due to angle of attack) are nonlinear with respect to control parameters such as angle of attack, sideslip, delta-aileron and delta-horizontal-pitch-trim. These aerodynamic vectors are used in determining the integrated aerodynamic load corresponding to a given maneuver simulation. Maneuver simulations are performed using a nonlinear iterative algorithm that computes control parameter angles necessary to satisfy equilibrium conditions about the vehicle's center of gravity. The algorithm is iterative because it is interpolating on the aerodynamic pressure vectors representing the control parameter states closest to the current trim parameter prediction. An example integrated aerodynamic load is depicted in (1), where each term represents the contribution of onset-

flow, control surface, rotary rate, and acceleration parameters, respectively.

$$\begin{aligned}
 \text{Lift} = & P_{L_0} + \frac{\partial P_L}{\partial \alpha} \alpha + \frac{\partial P_L}{\partial \beta} \beta \\
 & + \frac{\partial P_L}{\partial \delta_E} \delta_E + \frac{\partial P_L}{\partial \delta_A} \delta_A + \frac{\partial P_L}{\partial \delta_R} \delta_R \\
 & + \frac{\partial P_L}{\partial P} P + \frac{\partial P_L}{\partial Q} Q + \frac{\partial P_L}{\partial R} R \\
 & + \frac{\partial P_L}{\partial N_x} N_x + \frac{\partial P_L}{\partial N_y} N_y + \frac{\partial P_L}{\partial N_z} N_z \\
 & + \frac{\partial P_L}{\partial \dot{P}} \dot{P} + \frac{\partial P_L}{\partial \dot{Q}} \dot{Q} + \frac{\partial P_L}{\partial \dot{R}} \dot{R}
 \end{aligned} \tag{1}$$

At the equilibrium state of the vehicle in a maneuver (e.g., 9g symmetrical pull-up or 5.86g asymmetric rolling pullout), inertia forces are balanced with aerodynamic forces at the current control parameter values. The accuracy of the flight loads is highly dependent on the accuracy of each component of aerodynamic load. The Loads engineer endeavors to create a database where each aerodynamic pressure vector is correlated to physically known quantities. The large database provides an environment for expedient computation of thousands of flight maneuver simulations surveying the flight envelope for critical component design loads.

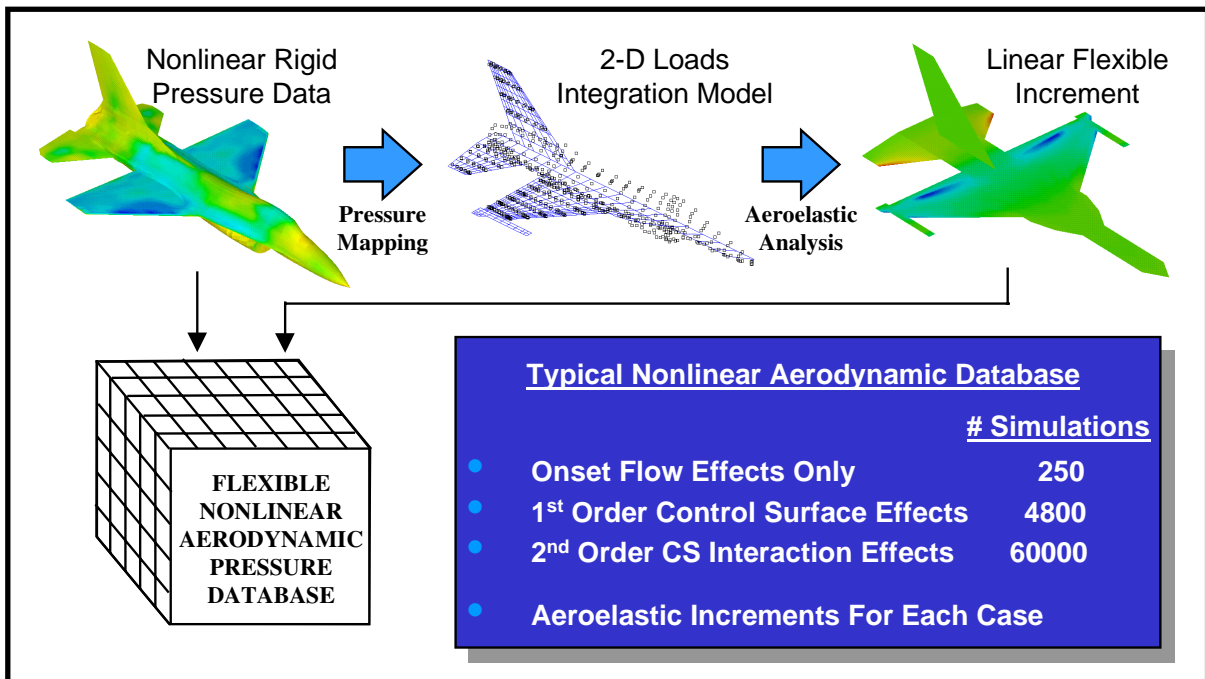


Figure 2: Construction and topology of a nonlinear aerodynamic database for fighter loads

The flight loads regime for high performance fighter aircraft consists of moderately high angles of attack (8-15 degrees) in transonic Mach numbers (0.8 – 1.2). Angles for control surfaces may range from +30 degrees to –30 degrees. The resulting aerodynamic flow regimes include complex shock interactions, flow separation, and other nonlinear flow phenomena.

Conventional methods of static aeroelasticity combine nonlinear rigid aerodynamic data (correlated to test) with linear flexible pressure increments derived using linear aerodynamic panel methods. These computations are depicted in (2) and (3), where the linear aerodynamics is introduced through an aerodynamic influence coefficient matrix, [AIC], and corresponding spline matrices, [G], to allow solutions in the structural domain. Structural displacements, {u}, are calculated in the equilibrium equation (2) combining mass, [M], stiffness, [K], and rigid nonlinear load {P_{NL}}. The aeroelastic increment is computed in (3) using the resulting structural displacements. The depicted example pertains to a solution for a nonlinear pressure increment at angle of attack.

$$[\mathbf{M}]\{\ddot{u}\} + [\mathbf{K}]\{u\} - \bar{q}[G^p][AIC][G^d]\{u\} = \{P_{NL}(\alpha)\} \quad (2)$$

$$\{P_{NL}(\alpha)\}_{increment} = -\bar{q}[G^p][AIC][G^d]\{u\} \quad (3)$$

Computational aeroelasticity enables a departure from the linear static aeroelastic analysis process by removing the aerodynamic influence coefficient approximation. This should improve accuracy, reduce risk and cost through avoidance of repair or even redesign for aircraft components of the operational flight vehicle. Limiting factors such as computational cost and the learning curve with respect to applying the CFD solver in an aeroelastic solution preclude wholesale adoption of the method.

Historically grid generation and re-generation impeded the process for computational aeroelastic analysis. Several applica-

tions in the literature have shown reliable results for standard test-bed problems (lifting surfaces in transonic flows) [5-11]. Analysis time for each of these codes must consider initial grid generation, and in the case of complex geometry, modeling may require significantly more time than the actual solution. Recall that databases for the fighter aircraft include a large distribution of onset flows multiplied by control surface settings. Each control surface survey may require a change of geometry up to plus and minus thirty degrees (transpiration methods are limited). Complex geometry considerations, such as external stores, may require over-set grids as well.

All of the mentioned codes rely on grid-moving techniques to couple the nonlinear aeroelastic equations. Common techniques noted use interpolation and dynamic mesh (pseudo-structural) methods and are applied to structured grid and unstructured grid codes. Geometric conservation laws are incorporated to maintain energy in the total system. These techniques allow for dependable regeneration of the aeroelastic solution. However, model re-gridding (e.g., grid adaptation) may be necessary to capture true aeroelastic phenomena.

A desire to rapidly capture aeroelastic phenomena with full airframe geometry motivated a probe to incorporate Lockheed Martin Aeronautics Company's SPLITFLOW [1] into a loosely coupled aeroelastic analysis method. SPLITFLOW (Figure 3) is an unstructured Cartesian prismatic grid

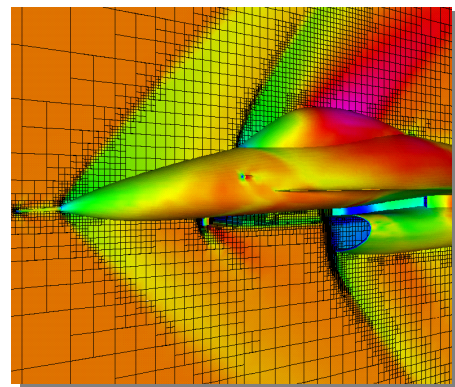


Figure 3: SPLITFLOW solution demonstrating automated and adaptive gridding

code. The unstructured Cartesian grid is primary, and is automatically generated using recursive cell subdivision. This grid scheme enables rapid and dependable Euler solutions for complex geometry. The secondary grid system, using triangular prismatic elements, may be added for resolving the boundary layer region near surfaces of solid bodies for Navier-Stokes analyses.

A process of associating Cartesian grid cells to triangulated surface facets generates the SPLITFLOW grid. The surface facets, defined by the user, are sufficient to describe the aerodynamic geometry with respect to expected flow features. Subsets of the facets comprise boundary elements (e.g., leading edge flap), and facilitate rapid geometry changes. The code uses an octree algorithm in minimizing cells while adapting to flow gradients. SPLITFLOW's cell division and cutting process relate surface facets to the Cartesian grid and establishes the solution boundary conditions. Grid refinement at each solution-iteration is controlled to user-defined regions and by user-defined flow quantities including velocity magnitude, Mach number, and pressure.

This paper presents a unique approach that updates the fluid-structure interaction solution at each aeroelastic iteration by recutting the Cartesian grid. The grid remains stationary while the structure (i.e., SPLITFLOW facets) passes through the flow field. The grid is derefined and refined around the new position at each iteration using SPLITFLOW's Cartesian grid cell cutting approach. A prototype tool developed to demonstrate feasibility illustrates the approach for a typical fighter aircraft. A commercial-off-the-shelf (COTS) approach is being built with the MDICE [2] procedure to provide capability for production aircraft analysis. Verification and validation studies are presented and discussed. A full-up aircraft analysis is presented and discussed.

2 Prototype Tool

A prototype aeroelastic analysis capability was developed by loosely coupling SPLIT-

FLOW to a simple structural deflection module. The deflection tool was based on libraries and methods developed in another effort linking NASA Langley's CDISC aerodynamic shape design to SPLITFLOW. The prototype capability provides for one flexible surface.

The general algorithm starts with a rigid baseline solution. Using the definitions of the surface facets, the computed pressure coefficients are integrated to the structural mesh, defined by a list of nodes and element node connectivity. In this case, the loads were integrated from the aerodynamic mesh by simply allocating each triangle's load to the nearest structural node.

A direct structural flexibility matrix derived in MSC.NASTRAN is used to solve for the structural deflections by simply multiplying the integrated nodal load vector. Each structural node deflection is used in building a NURBS surface with DT_NURBS interpolation. Each node on the faceted aerodynamic surface is projected to the NURBS surface to compute its deflection. Deflections are applied to the SPLITFLOW facet nodes with a relaxation factor between 0.0 (no deflection) and 1.0 (no relaxation). Values around 0.1 have shown to obtain smooth aeroelastic convergence.

Using the new aerodynamic surface, SPLITFLOW is restarted, recutting the grid and continuing the solution process. When the loads and deflections have stopped changing significantly (in practice, nodal deflections converged to .001") and the CFD solution itself is determined "mature" (with judgment left to the user), the run is complete. The static aeroelastic solutions are not time-accurate solutions, and geometric conservation is implicit in the small relaxation factors. More discussion is provided in the validation studies following.

In practice, an F-16 type analysis under high-g symmetric pullup flight conditions (see Figure 4), requires approximately 3,000 CFD iterations, 30 aeroelastic iterations, with 75-100 CFD iterations in between each aeroelastic iterations, and grid adaptations

each 25 iterations or so. On a 16-processor HP V2500 supercomputer, the entire process takes about three to four days.

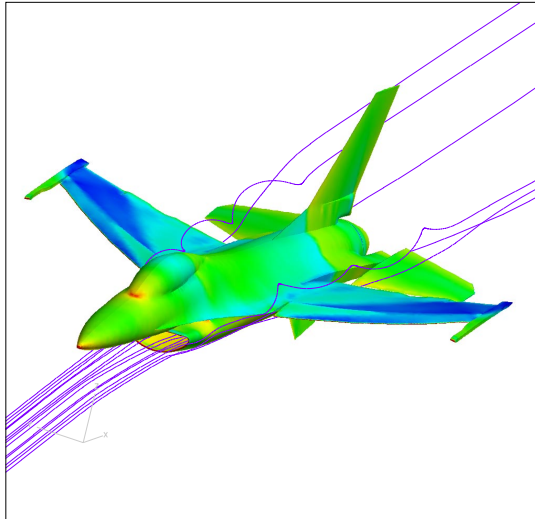


Figure 4: SPLITFLOW facets updated with structural deflections

This capability has been applied to the F-16 Conformal Fuel Tank (CFT) design. In particular, it has been used in studies to examine reduction in wing load and pitching moment provided by flaperon uprig under high aeroelastic loads. This was an important study because flaperon uprig is already used to decamber the wing for load alleviation, and the addition of the CFT creates increased body camber with resultant increases in lift and pitching moment. A key feature was the reuse of the exact procedure and aeroelastic coupling developed for the prototype demonstration. The geometry peculiar to the CFT configuration and control surface deflections simply replaced associated F-16 data with no additional user interaction required than the prototype case. Insertion into existing methods in Aerodynamics and Structural Analysis is a primary goal of this R&D effort.

3 Aeroelastic Methodology

A typical fighter aircraft is completely flexible with multiple control surfaces that rotate and deflect in non-integral shapes. The deflection and discontinuous nature of aerodynamic loads impose requirements for

modeling of discrete fluid-structure interface components (i.e., for aileron, wing box, leading edge flap, forward fuselage, empennage, etc.). Provision of COTS tools for core structural finite element analyses is required. Specifications for a loosely coupled aeroelastic analysis environment led to use of MDICE, integrating SPLITFLOW and structural finite element data.

MDICE provides for conservative and consistent mapping of multiple fluid-structures interaction components through several methods [2] as well as integration with COTS structural finite element codes. MDICE provides an environment that handles the transmission of data between disciplinary modules across networks and computing platforms. Data transmission occurs through memory; therefore providing simulation composed of separate analyses distributed across a heterogeneous network and appearing as a tightly coupled code. Existing analysis codes are integrated through an object-oriented application programming interface (API), ensuring that modern technology can readily be implemented into the simulation process. Once integrated (deemed MDICE-compliant), analyses are coordinated in a multidisciplinary simulation through a scripting language. The prototype approach has been integrated into MDICE (Figure 5). The disciplinary analyses are initiated from within MDICE. Each analysis loads grid and restart information and then, releases execution control to MDICE. Once each module is placed in a wait mode, the simulation is run through the scripting language, which is executed through the MDICE GUI. The first command usually issued to each module creates an interface object within MDICE. An interface object stores pointers to the grid and variable information that resides directly in the analysis module's memory. Following, MDICE assembles the interface objects, or performs calculations necessary for the interpolation of quantities between the disciplinary grids. For the purpose of the reported studies, the method of Brown [12]

Using the MDICE/SPLITFLOW environment, solutions have been obtained to date for both concepts at Mach 0.9, simulated 10K altitude, and a simulated 9g pull-up condition (~8.9 degrees AoA). Measured structural influence coefficient data was acquired in the VAT program for both concepts and used in these aeroelastic analyses. The solution for the washout concept has been subject of previous studies [9], and an Euler solution was obtained without much trouble. The solution for the washin concept was difficult to obtain and requires a full Navier-Stokes solution which was not complete at the time of this paper.

4.1 Washout Wing Solution

The washout wing exhibits the largest deflections of the two aeroelastically tailored concepts. The local angle of attack of the cross-sections is reduced as the wing deflects, and the flow remains attached over the entire wing. As a result, the Euler equations are successful in capturing the flow characteristics of the washout wing.

Figure 7 displays the aeroelastic pressure distributions obtained from SPLITFLOW/MDICE. The results match very well with experimental data. The C_p distributions near the wingtip display classical Euler treatment of the viscous phenomenon. The first major difference between the predicted and experimental results is that the shock strength is much higher in the predicted pressure distribution. This is due to a lack of viscosity in the Euler analysis. In areas where the effects of viscosity are less noticeable (i.e. from midspan to the wing root) the correlation between the predicted and experimental results increases greatly.

Figure 8 displays a deflection summary for the washout wing. The deflections obtained from SPLITFLOW / MDICE matched the experimental loads very closely. The predicted deflection at the tip of the leading edge spar was 3.03 inches, while the experimental deflection at the same location was 3.01 inches. This results in an error of 0.66%. The predicted and experimental twist

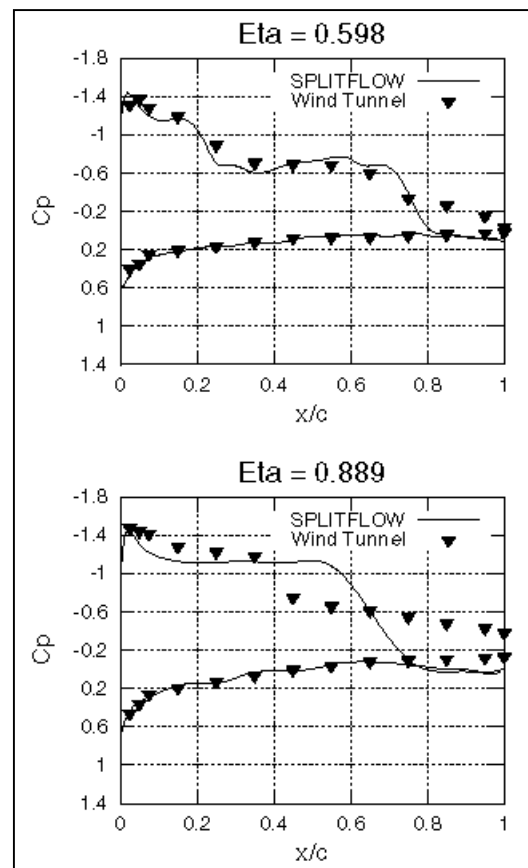


Figure 7: Washout Euler solution agrees well – over predicts shock strength

distributions (Figure 9) for the washout wing exhibit a smaller amount of twist for the predicted data that is most likely due to the loss of aft loading caused by the strong shock.

Figure 10 exhibits a history of convergence vs. iteration. Applied deflections, total calculated deflection, and force at the tip of the leading edge spar were monitored throughout the simulation. The figure also illustrates how the amount of applied deflection is controlled by the relaxation factor. By the relaxation factor, the applied deflection approaches the total calculated deflection in an asymptotic manner. At the discretion of the user, the relaxation factor is increased to accelerate the convergence.

While the Euler solution provides excellent agreement in the washout case, improvement is expected with a Navier-Stokes solution. At the time of this paper, a Navier-Stokes solution had not been obtained.

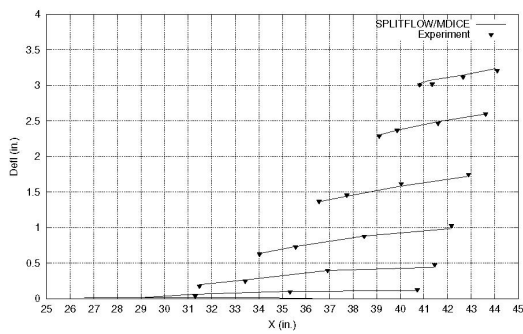


Figure 8: Washout deflections exhibit aeroelastic twist

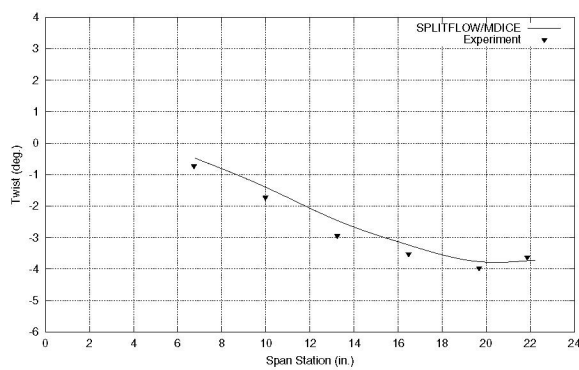


Figure 9: Analytic twist distribution is under-predicted due to loss of aft loading

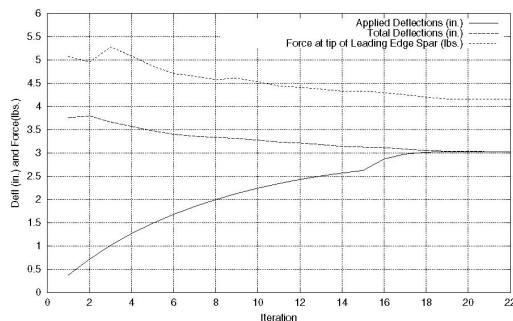


Figure 10: History shows monotonic convergence of displacement and force

4.2 Washin Wing Solution

The washin wing solution contrasts greatly with the washout wing solution. The wing planforms and aerodynamic flow conditions are identical. Due to the increase in angle of attack of the wing sections inherent in the washin concept, the flow separates on the outboard section. Although there is no direct attempt to model the viscous properties of the fluid that allow separation to occur, there is enough numerical dissipation to give the flow solver “viscous-like” properties. The

numerical dissipation acts as a pseudo-viscosity. An increase in grid density might alleviate the effect.

Often, the loads engineer has to tackle a problem with physics that are adequate, instead of appropriate. In the context of SPLITFLOW, employing the Euler equations to solve problems of this type means judging the amount of dissipation introduced by the numerical scheme. The amount of dissipation introduced is inversely related to the density of the Cartesian grid, i.e. the higher the grid density, the less dissipative the flow is in that vicinity. This introduces an interesting tradeoff between trying to obtain a viscous-like solution and maintaining accuracy. Consequently, management of the grid adaption also plays an even more important role. Periodic benchmark tests with the appropriate physics are also useful.

A second issue that arises is determining a suitable criterion for convergence during an aeroelastic cycle. This is not as simple as allowing the solution to converge until the residuals have been reduced by two orders of magnitude. When approaching problems in this manner, it is best to be conservative, allowing the Euler equations enough time to resolve the major features of the solution that may appear during the current iteration. Upon the onset of separation, the number of CFD iterations performed per aeroelastic cycle was doubled in order to allow the region of separation to develop.

Figure 11 shows the C_p distributions obtained from the washin aeroelastic simulation. Similar to the washout wing, the C_p distribution agrees well with the inboard section, but begins to differ as the wingtip is approached. The solution obtained for SPLITFLOW / MDICE predicted a smaller region of separation than exhibited in the experimental data. The result is higher loads and greater deflections. Figure 12 displays the predicted and experimental deflections. Because the separation patterns are not accurately captured, the twist distribution near the wingtip clearly differs from

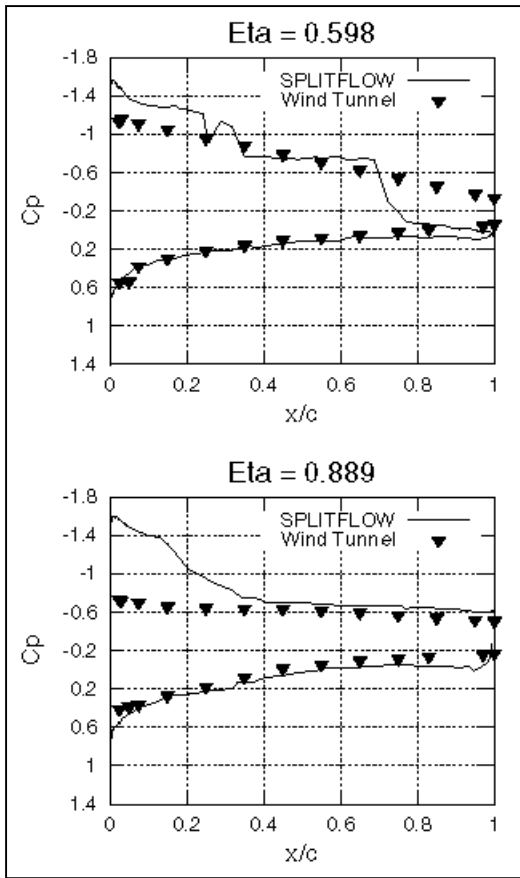


Figure 11: By numerical dissipation, Euler solution approaches experiment

experimental data (Figure 13). The importance of relaxing the applied deflections is evident in Figure 14, where it is seen that the unrelaxed deflections temporarily reached a much higher value than the final deflection. Lastly, Figure 15 illustrates the differences in the separation patterns that appeared in the wind tunnel and in the SPLITFLOW solution. This solution exhibits features of unsteady flow that illustrate the need for a viscous solution, which is being pursued.

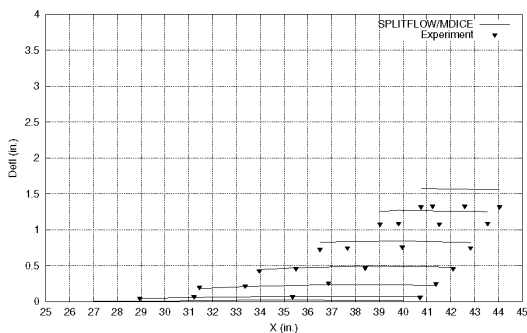


Figure 12: Washin deflections overpredicted due to inability to accurately predict flow separation

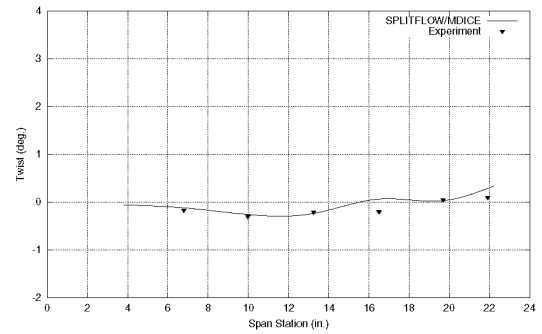


Figure 13: Analytical twist distribution indicative of remaining attached flow

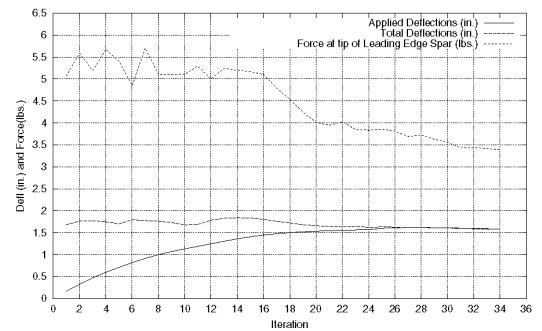


Figure 14: Unsteady nature of flow exhibited in convergence history

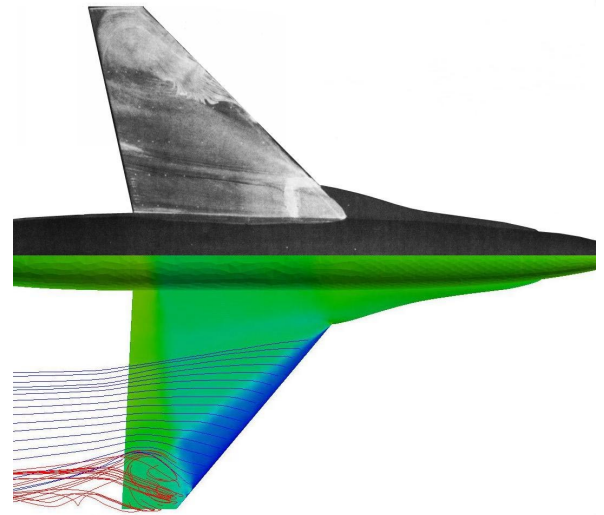


Figure 15: Comparison of wind tunnel and CFD flow visualization results showing the differences in separation patterns.

5 F-16 Integrated Analysis

Upon completion of verification and validation testing of the MDICE / SPLITFLOW environment with Euler solutions, an integrated test was run for a typical fighter

aircraft with multiple control surfaces. In this simulation an Euler solution is obtained for a full F-16 geometry coupled with a structural finite element model. Solutions obtained within the prototype system mentioned previously, uses a single surface for the entire wing (wing box, leading and trailing edge flap) and launcher to map CFD pressures to the structural grids and structural deformations to the CFD geometry. In this case, individual component mappings are defined to prevent incorrect translation of loads and displacements between components. For instance, the leading edge flap on the CFD model is mapped with the leading edge flap on the structural finite element model. Independent mapping is important to capture the correct physical behavior of each component (i.e., leading edge flap rotation and deflection as it is attached to the wing box).

Figure 16 displays the component mappings defined for this analysis. Individual mappings are defined for the wing box,

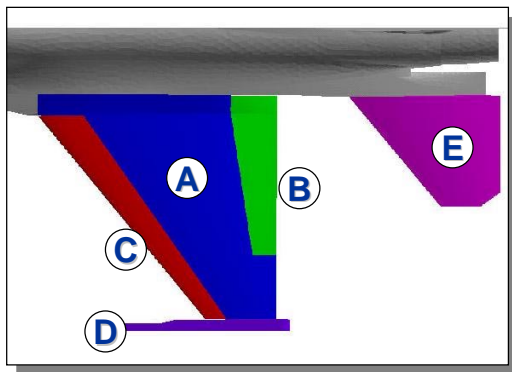


Figure 16: Discrete components are mapped for translation of loads and displacements

leading edge and trailing edge flaps, the missile launcher, and the horizontal tail.

Figure 17 exhibits the component behavior that is desired. Notice that the trailing edge flap is “blowing back.” With the single surface approach of the prototype, such resolution between a control surface and the wing box is not available.

Figure 18 displays the results of the solution for the F-16. The flight condition is for a Mach 0.9, 10,000 ft max-g pullup. Since the wing behaves as a washout wing, the solution progressed similarly to the washout test case discussed previously. The solution was run on a loaded HP V class supercomputer using a little more than four processors in parallel over the course of eight days. Notice in the figure that the vortices off of the strakes are wrapping around the vortices off of the launcher. The total wing deflections correlate with similar solutions from the prototype tool. Further correlation with flight test data is being acquired.

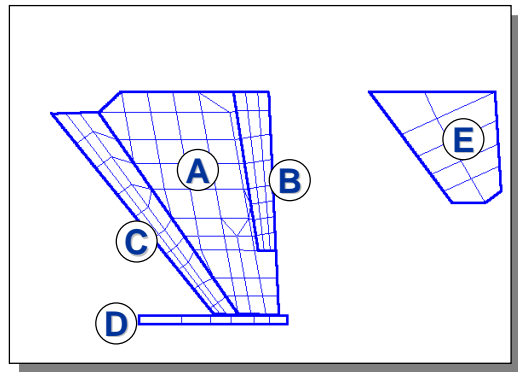


Figure 18: F-16 static aeroelastic solution for transonic flight condition

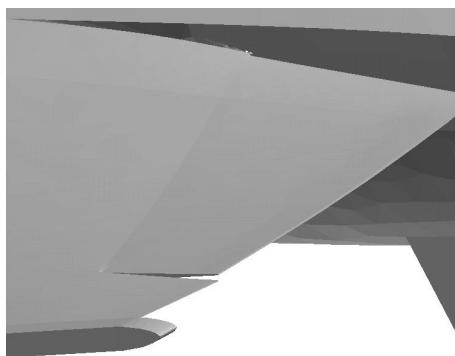
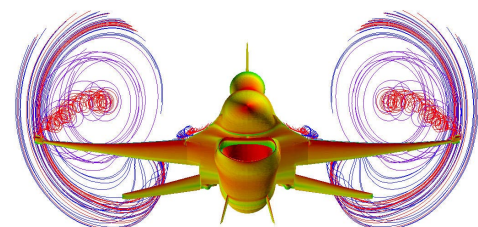


Figure 17: Trailing edge “blow-back” from aeroelastic solution



6 Summary

A new method for computational aeroelastic analysis is presented that provides for timely analysis for complex geometry. The presented technique uses a Cartesian grid scheme that allows the mesh to be automatically generated and adapted in each aeroelastic iteration. The solution scheme moves the geometry facets through the Cartesian mesh at each aeroelastic iteration as opposed to common methods where the entire mesh is deflected to accommodate the deformed vehicle geometry. The presented scheme provides an alternate method for computing static aeroelastic pressures that can be used in development of critical flight loads. Studies have shown a requirement for continued development and validation of a viscous capability. Current efforts are focused in this area.

References

- [1] Siegel J M, Jr., et al. Application of a Multi-Disciplinary Computing Environment (MDICE) for loosely coupled fluid-structural analysis. Presented at the 7th AIAA/USAF/NASA/ISSMO Symposium of MDO, AIAA 98-4866, September 1998.
- [2] Karman S L Jr. SPLITFLOW: 3d unstructured cartesian/prismatic grid CFD code for complex geometries. American Institute of Aeronautics and Astronautics Paper, AIAA-95-0343.
- [3] Love Michael H, et al. Enhanced maneuver airloads simulation for the automated structural optimization system, ASTROS. American Institute of Aeronautics and Astronautics Paper, AIAA-97-1116.
- [4] Neill D J, and Sikes G. The MSC Flight Loads System. MSC Aerospace User's Conference, November 1997.
- [5] Luker Joel J, Huttshell Lawrence J. Air Force Research Laboratory's progress in fluids-structures interaction. American Institute of Aeronautics and Astronautics Paper, AIAA-98-2420.
- [6] Bennett Robert M, Edwards John W. An overview of recent developments in computational aeroelasticity. American Institute of Aeronautics and Astronautics Paper, AIAA-98-2421.
- [7] Hartwich Peter M, and Agrawal Shreekant. Method for perturbing multiblock patched grids in aeroelastic and design optimization applications. American Institute of Aeronautics and Astronautics Paper, AIAA 97-2038.
- [8] Lee-Rausch Elizabeth M, and Batina John T. Calculations of AGARD wing 445.6 flutter using Navier-Stokes aerodynamics. Presented at the American Institute of Aeronautics and Astronautics 11th Applied Aerodynamics Conference, AIAA 93-0001, August 9-11, 1993.
- [9] Schuster D, Vadyak J, and Atta E. Static aeroelastic analysis of fighter aircraft using a three-dimensional Navier-Stokes algorithm. Presented at the 28th American Institute of Aeronautics and Astronautics Aerospace Sciences Meeting, AIAA 90-0435.
- [10] Guruswamy G P, Byun C. Fluid-structural interactions using Navier-Stokes flow equations coupled with shell finite element structures. Presented at the 24th American Institute of Aeronautics and Astronautics Fluid Dynamics Conference, AIAA 93-3087, July 6-9, 1993.
- [11] Farhat Charbel. High performance simulation of coupled nonlinear transient aeroelastic problems. *Parallel Computing in CFD*, AGARD-R-807, October 1995.
- [12] Brown S A. Displacement extrapolations for CFD+CSM aeroelastic analysis. American Institute of Aeronautics and Astronautics Paper AIAA 97-1090, 1997.
- [13] Rogers W A, et al. *Validation of aeroelastic tailoring by static aeroelastic and flutter tests*. AFWAL-TR-81-3160, September 1982.